ISSN 1392-1207. MECHANIKA. Vol. 31, No. 4, 2025: 368–376

Experimental Investigation of Suspended Water, Ethanol and Acetone Droplets Transient Phase Change Regimes in the Heated Airflow

Kristina BIKNIENĖ
Kaunas University of Technology, Studentų 56, Kaunas, LT-51424, Lithuania, E-mail: kristina.bikniene@ktu.edu
https://doi.org/10.5755/j02.mech.41762

Nomenclature

c_p – specific isobaric heat, kJ/(kg K); G – mass flow rate, kg/s; g_v – vapour mass flux, kg/s; L – latent heat, kJ/kg; p – pressure, Pa; R – radius of droplet, m; $2R$ – diameter of droplet, m; Re – Reynolds number; t – temperature, °C; X_v – vapour volume fraction in gas mixture; V – volume, m^3; ΔV_l – liquid volumetric change rate, m^3/s; ρ – density, kg/m^3; τ – time, s; λ – thermal conductivity coefficient, W/(m K); φ – relative humidity, %;

Subscripts: a – atmospheric; co – condensation; dp – dew point; e – equilibrium evaporation; eq – equivalent; f – phase change; g – gas; i – time index; k – conductivity; l – liquid; m – mass average; n – frame sequence number in the time of one second; N – amount of frame numbers per one second; s – saturation; TB – thermocouple bead; TW – thermocouple wires; v – vapour; vg – vapor-gas mixture; 0 – initial.

1. Introduction

The application of liquid spray in technologies used in the energy, transport and various industrial sectors is extensive. Traditional examples include the liquid fuels used in internal combustion engines and industrial boilers [1-6], water spraying in fire suppression [7-10], air-conditioning systems [11-13], and gas cooling [14,15]. In today's technology, the liquid spraying process is widely used to increase energy efficiency and reduce environmental pollution. For example, in modern biofuel combustion technology, water and condensate are sprayed to humidify the solid fuel before burning, to cool the combustion products before the condensing economiser, and to reduce pollutant emissions in the flue gas [16-19]. With the booming of high-power electronics and high-efficiency energy conversion, the efficient removal of large amounts of waste thermal energy from small spaces has now become a significant issue. This can also be achieved through liquid spraying, which ensures high heat flux removal and precise temperature control [20-24].

The widespread use of liquid spray-based technologies is attributed to their efficient heat and mass transfer capabilities. Spraying breaks up the liquid into small droplets and greatly increases the contact area between the liquid and gas phases. This determines the rapid heat and mass transfer processes, the intensity of which is directly related to the analysis of the variation of the thermal state of the single droplet and the phase change processes occurring on its surface. The heat and mass transfer processes between the droplet and the surrounding gaseous environment are strongly influenced by the complex transfer interactions, which are manifested by the effects of Stefan hydrodynamic flow, droplet slipping in the gas flow, selective radiation, and other factors. Therefore, to ensure optimal boundary conditions for the specific spray-based technology, it is essential to thoroughly understand the complex heat and mass transfer mechanisms in a single liquid droplet and to control them properly. The investigation of this problem is known in the scientific literature as the “droplet” problem and has been of interest to researchers in various fields for more than a century [25]. Due to its wide application in various fields and the diverse range of complex heat and mass transfer boundary conditions in specific technologies, the high level of interest in this topic remains relevant today [26].

The heat and mass transfer of sprayed liquid droplets can be analysed using a single droplet phase change regime cycle diagram (Fig. 1). It schematically illustrates how a heated liquid droplet behaves and the connection between the variation of the thermal state and the diameter of the droplet. The beginning of the sprayed droplet phase change is determined by the moment $\tau = 0$ and the end of the droplet evaporation cycle is $\tau = \tau_f$. When the initial temperature of the liquid droplet $t_{l,0}$ is lower than the surrounding air dew point temperature t_{dp}, the droplet first warms, and its diameter grows: condensation process of water vapour from the air takes place on the droplet’s surface. Additionally, the liquid's thermal expansion contributes to the growth in size of the liquid droplet. It is a condensation regime. When the droplet temperature t_l becomes higher than the temperature t_{dp}, the evaporation process begins: the droplet’s diameter $2R_l$ decreases, but the temperature t_l still grows. It is a transient evaporation regime. When the temperature of the droplet reaches the t_e temperature at which the equilibrium evaporation regime begins, the droplet's thermal state remains almost unchanged, and the droplet’s diameter reduces according to the diameter-squared law.

The equilibrium evaporation regime is the most investigated. This is because in traditional spray-based technologies, it is essential how quickly the sprayed droplet evaporates. The results of experimental studies conducted by various authors with water droplets in the equilibrium evaporation regime are summarised graphically [27]. These conducted experiments have shown that in the equilibrium evaporation state, the entire heat transferred to the surface of the droplet is used to evaporate the water, and the heated droplet temperature t_e depends on the surrounding gas temperature t_g but is lower than the saturation state temperature of the gas t_s. In today's liquid spray-based technologies, such as low-temperature spray cooling in electronic devices or waste heat recovery from humid biofuel gas, transient phase change regimes are essential. During the initial processes of transient phase change, the most intense heat and mass transfer processes between the droplet and the surrounding gas can take place, which determines the efficiency of the

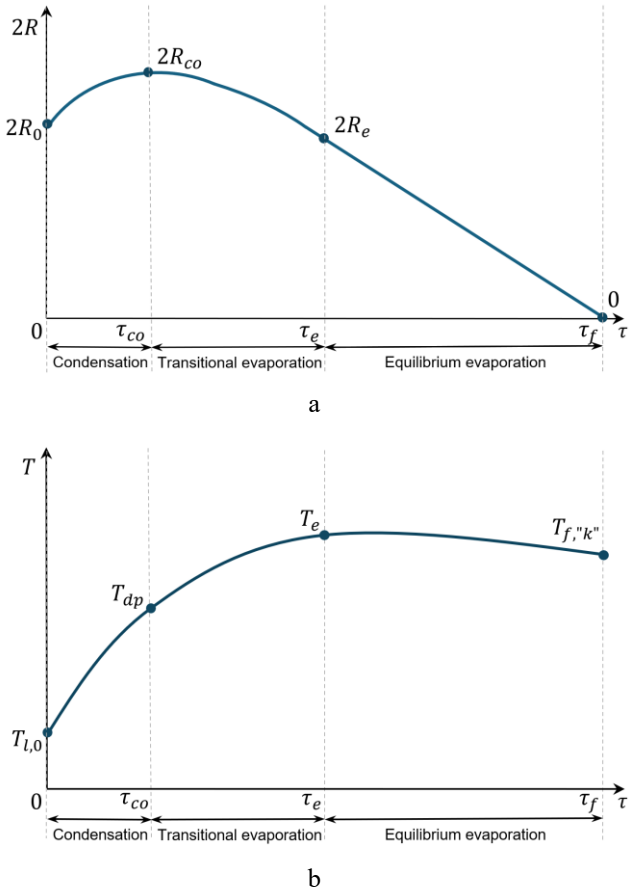

Fig. 1 Phase change regime cycle diagrams of single pure liquid droplet (when $t_{l,0} < t_{dp}$): a – diameter $2R_l$ variation, b – temperature t_l variation

mentioned technologies. This leads to an increasing focus on the initial stages of phase change in recent research work on droplets [27-33].

Modern optical measurement techniques such as particle image velocimetry (PIV) [29] and laser-induced fluorescence (LIF) [28, 30] are now widely used in experimental studies of liquid droplets. These are non-contact measurement methods with high speed and accuracy. They operate by adding dyes or particles to a liquid, illuminating the liquid with laser light, and recording the intensity of the dye or particle emission. The contact temperature method, combined with video recording, is also employed to investigate the heat exchange and phase change processes in heated liquid droplets. Here, the liquid droplet is directly suspended on the thermocouple bead, and the experimental droplet temperature is measured. For example, this measurement method for droplet parameters is used in experimental studies [27, 32]. These papers investigate the heating and evaporation processes of water droplets in the air flow with temperatures characteristic of the condensing economiser in biofuel technologies. The results indicate that the humidity of the gas flow influences the heat and mass transfer processes in a heated water droplet, particularly in the initial stages of phase change. It was also found that the initial temperature of the sprayed water affects the characteristics of the droplets' transient phase change regime. In these experiments, during the equilibrium evaporation regime, a noticeable increase in the temperature of the water droplet was recorded. This may have been affected by additional heat input to the suspended droplet through the thermocouple wires. Moreover, the issue of synchronising droplet temperature measurement with filming remained, raising questions about possible uncertainty in the droplet's initial parameters. However, this did not hinder the study of the trends related to the influence of airflow and additional humidification on the entire phase change regime cycle of the water droplet. Nonetheless, to study the transient regimes of the droplet in more detail, it is necessary to refine this experimental method.

In experimental studies on liquid droplets, water is the most commonly used test fluid because of its widespread application in various spray-based technologies. However, to ensure greater efficiency of heat and mass processes in modern equipment, whose operating conditions are becoming increasingly diverse, efforts are now being made to use alternative liquids, such as ethanol and acetone, without increasing the device's size. For example, ethanol and acetone can be used in spraying the cooling system to intensify the removal of excess heat and to control the surface temperature of the cooled device itself [34-37]. Both ethanol and acetone can be blended as additives into fossil fuels to reduce emissions [38, 39] or into biofuels to enhance combustion properties [40, 41].

This work aims to experimentally investigate the influence of surrounding airflow temperature on the transient heat and mass transfer processes of water, ethanol and acetone droplets in the initial stages of their phase change. This paper also presents experimental diagrams of the droplet temperature changes and equivalent diameter variations of the investigated liquids, as well as the dynamics of the liquid volume change rate of experimental droplets during the transient phase change.

2. Experimental Method and Processing of the Results

The experiments were conducted in an experimental setup, the general view of which is presented in Fig. 2. The principal scheme and detailed operation description of the experimental setup are provided in the studies [27, 32, 42]. The main constructive components of the setup are two consecutively connected electrical heaters of atmospheric air, a water vapour generator and a vertical experimental section. The experimental droplet is suspended on the thermocouple bead using a mechanical pipette. Then, with a special introduction system consisting of two sliding glass tubes, it is placed at the centre of the experimental

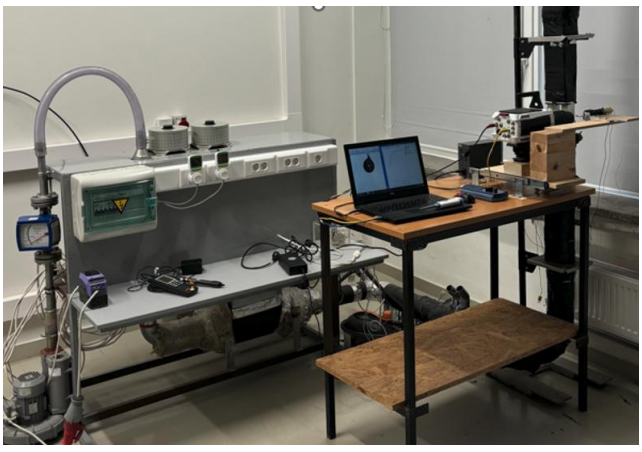

Fig. 2 General view of the experimental setup

section. Then, the protective tube is withdrawn, and the supplied air flow is directed directly over the experimental liquid droplet. The main observed parameters of experiments are the temperature (measured at 0.1 s) and the size of the droplet, which is filmed with a Phantom V711 camera at 25 frames/s. The TESTO 445 instrument measures the relative humidity, temperature and pressure of the supplied atmospheric air with accuracies of ± 2% RH, ± 0.3 °C and ± 0.1 kPa respectively.

To study the transient regimes of the droplet in more detail, the experimental equipment was modified. This improved the quality and reproducibility of the experimental results. The current thermocouple used to measure the temperature of a liquid droplet is the T-type thermocouple, which has higher characteristics: its accuracy is 0.5°C and its thermal delay is 0.1 s. The wires used in this thermocouple are only 0.12 mm in diameter. Thus, the effect of the heat flowing through the wires on the heat and mass transfer processes of the suspended droplet is minimal and barely noticeable, so that it can be discarded in the initial stages of the phase change. The procedure for inserting the suspended liquid droplet into the experimental section was also redesigned. The droplet thermocouple insertion mechanism, the imaging camera and the light source were installed on a unified moving platform. This allows for the start of filming the experimental droplet from the moment it is suspended on the thermocouple. In this case, the droplet has not yet begun to warm or cool, and its measured parameters define the actual initial state. In addition, synchronous recording of the temperature and size of the experimental droplet is now available and ensured by software.

The data of the droplet's temperatures measured gives thermograms $t_l(\tau)$ of the heating process of liquid studied droplets. Although these experiments used thermocouples with smaller dimensions, in all cases an increase in the droplet temperature was detected during equilibrium evaporation. This shows that during equilibrium evaporation, the heat flowing through the thermocouple wires makes noticeable impact on the processes taking place in the droplet. Thus, in this paper, the analysis of the experimental results focuses on the initial stages of the droplet phase change. The video camera data are processed by an image recognition program, which outputs the results as a function of the variation of the droplet's equivalent diameter $2R_{eq}(\tau)$ (Fig. 3).

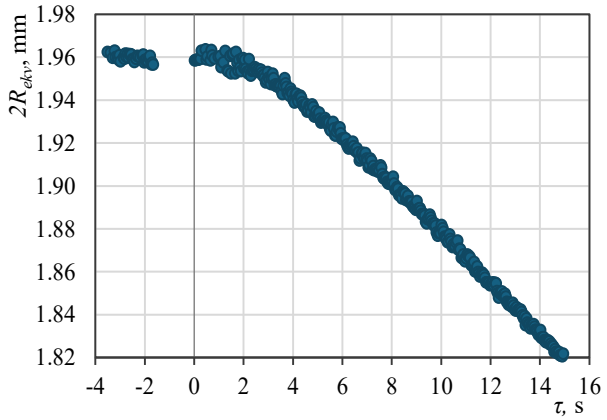

Fig. 3 An example of the instantaneous $2R_{eq}$ diameter variation of the water droplet in the initial stages of phase change under boundary conditions: $t_g = 130$°C, $X_{v,g} = 0.012$, $2R_{l,m,0} = 1.962$ mm, $G_g = 3.32$ g/s

The equivalent diameter of the experimental droplet is comprehended as the sphere's diameter of the combined volume of the liquid droplet, the thermocouple bead and the thermocouple wires immersed in the liquid. For a convenient analysis of the variation in the experimental droplet size, the average droplet diameter $2R_{l,m}$ is computed every second by evaluating the results of the instantaneous equivalent diameters of the N frames:

$$2R_{l,m} = \frac{\sum_{n=1}^{N} R_{eq,n}}{N}. \quad (1)$$

The experimental measurements' uncertainties are determined by the standard deviation of the main parameters' data, the accuracy of the measuring instruments, and the errors of the deduction itself, with a 95% level of confidence. Fig. 4 illustrates examples of droplet temperature and diameter with estimated measurement uncertainties. As in both cases, the measurement uncertainties are larger at the beginning of the experiment, and after reaching the equilibrium evaporation regime, their values decrease and become almost constant.

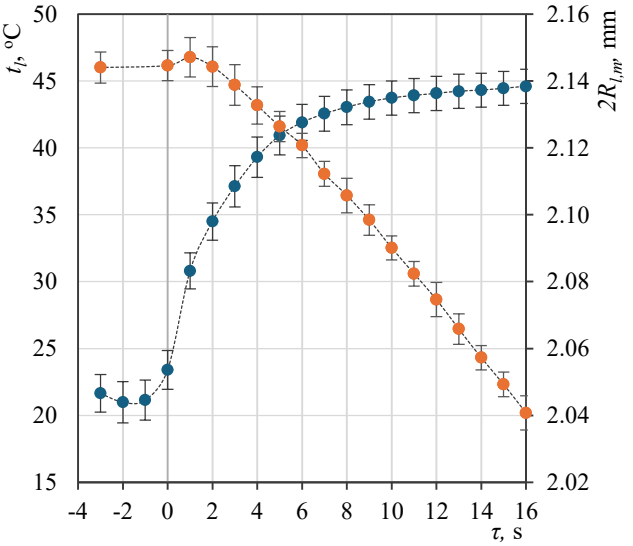

Fig. 4 The change of the experimental water droplet temperature t_l, and diameter $2R_{l,m}$ with the estimated measurement uncertainties in the initial stage of phase change; boundary conditions: $t_g = 100$°C, $X_{v,g} = 0.012$, $2R_{l,m,0} = 2.144$ mm, $G_g = 3.32$ g/s

In the engineering practice of liquid spraying, it is essential to know the evaporation rate of heated droplets. It indicated the rate at which phase changes occur in the droplet. It can be determined by the volumetric change rate and the vapour mass flux. Based on the experimental data obtained, a mathematical model was developed to determine these parameters. In the case under investigation, the droplet is composite, and its total volume is defined by the volume of the thermocouple bead V_{TB}, the volume of the liquid suspended on the bead V_l and the volume of the thermocouple wires immersed in the liquid droplet V_{TW}

$$V = V_{TB} + V_l + V_{TW}. \quad (2)$$

The volume of the heated composite droplet can vary due to expansion of the components due to their heating, phase change at the liquid surface (liquid evaporation

or liquid vapour condensation), and the immersion depth of the thermocouple wires. The influence of the thermocouple bead and the immersed thermocouple wires can be negated, then based on the experimental data, the liquid volume change rate ΔV_l can be estimated by calculating the change in the volume V of the composite droplet over a certain time:

$$\Delta V_{l,i>1} \approx \frac{V_i - V_{i\text{-}1}}{\tau_i - \tau_{i\text{-}1}} = -\frac{4}{3}\pi \frac{R^3_{l,m,i} - R^3_{l,m,i\text{-}1}}{\tau_i - \tau_{i\text{-}1}}. \quad (3)$$

The vapor mass flux of the experimental suspended droplet is defined by the mass variation in the phase change processes on the droplet's surface. From experimental data the instantaneous vapor flux in time interval can be calculated according to the following expression:

$$g_{v,i>1} = -\frac{4}{3}\pi \frac{\left[\left(\rho_{l,i} R^3_{l,m,i}\right) - \left(\rho_{l,i\text{-}1} R^3_{l,m,i\text{-}1}\right)\right]}{\tau_i - \tau_{i\text{-}1}}. \quad (4)$$

3. Experimental Results and Discussion

To investigate the influence of airflow temperature on heat and mass transfer processes occurring in droplets of different liquids during the initial stages of phase change, experiments were conducted at varying atmospheric airflow temperatures: 50°C, 100°C, and 130°C. These temperatures were chosen because they are often encountered in practical applications of low-temperature liquid spraying, such as in heat recovery for biofuel technologies and cooling electrical appliances. Water, ethanol and acetone have been used in the research. Their thermophysical properties are given in Table 1.

Table 1

Thermophysical properties of tested liquids at 20°C

Liquid	ρ	λ	c_p	L	t_s
	kg/m^3	W/(m·K)	kJ/(kg·K)	kJ/kg	°C
Water	998.2	0.598	4.186	2256	99.98
Ethanol	789.5	0.17	2.46	846	78.37
Acetone	790.1	0.16	2.15	518	56.08

During all experiments performed, the air flow of 10 m^3/h was supplied at $p_a \approx 105$ kPa, $t_a \approx 22$°C, and $\varphi_a \approx 50\%$ ($X_{v,a} \approx 0.012$). In all cases, the airflow regimes were transitional (Re_g=2870÷3180) in the experimental section. After just suspending the experimental droplets on the thermocouple, their diameters range from about 1.9 to 2.2 mm. The average initial droplet temperature for all liquids tested was the same as the ambient air temperature, approximately 22°C. However, as soon as the droplet is suspended, its temperature immediately decreases. The droplet size also changes slightly during the insertion process. These changes vary for each tested liquid and depends on its individual properties. As a result, the initial temperature and size of the droplet when it is placed in the experimental section differs from the values of these parameters at the time of droplet suspending. In the analysis of the experimental data, the temperature and diameter measurements of the liquid droplet are given from the moment the experimental droplet is in the centre of the experimental section. This time point is taken as initial $\tau \equiv 0$.

The measurement data of water droplet temperature are given in Fig. 5, a. As the data show, with increasing air temperature, the water droplet heats up more, and its equilibrium evaporation temperature t_e becomes higher. When the air is 50°C, the water droplet t_e is about 28.5°C. As the air temperature rises to 100°C and 130°C, t_e reaches almost 44.7°C and 50.4°C, respectively. This is because at

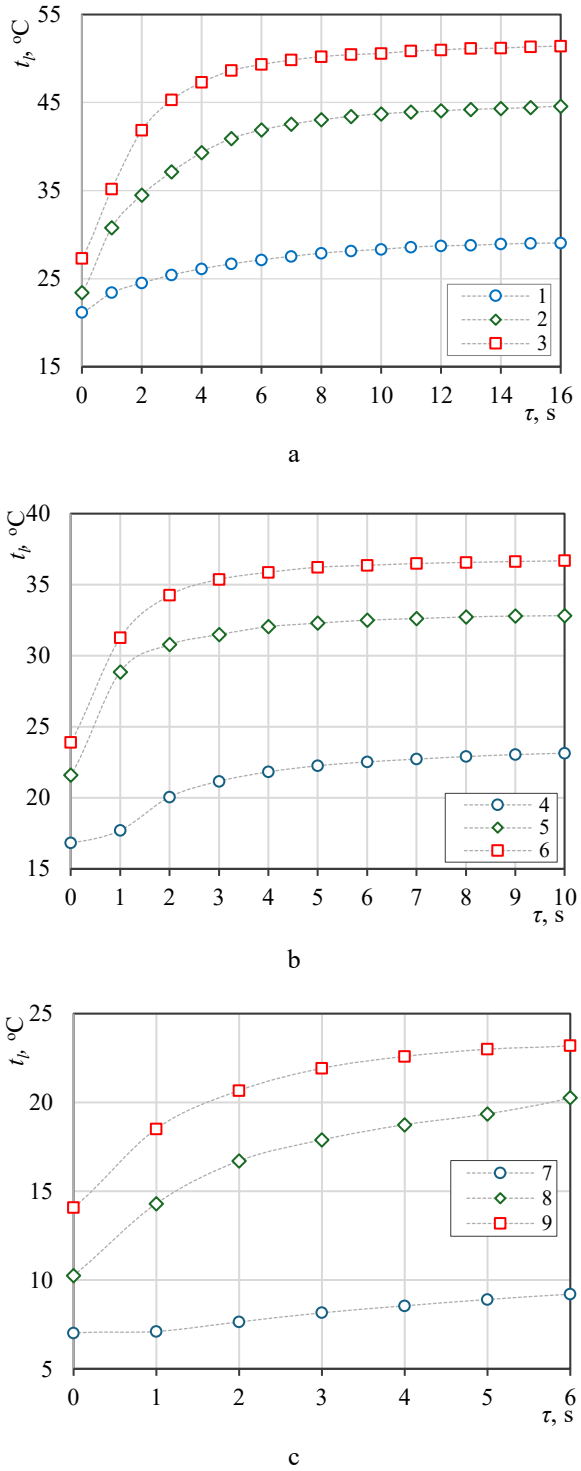

Fig. 5 The change of the experimental droplet temperature in the initial stages of phase change: a – water, b – ethanol and c – acetone; boundary conditions: t_g, °C: (*1,4,7*) 50, (*2,5,8*) 100, (*3,6,9*) 130; $X_{v,g}$=0.012, $2R_{l,m,0}$, mm: (*1*) 2.195, (*2*) 2.144, (*3*) 1.922; (*4*) 1.958, (*5*) 1.883; (*6*) 1.985, (*7*) 1.909, (*8*) 1.761, (*9*) 1.942; G_g=3.32 g/s

higher air temperatures, more intense liquid evaporation occurs, and therefore the balance of heat flows characteristic of the equilibrium evaporation regime is established at higher temperature t_e. Temperature data also demonstrates that at higher air temperatures, the thermal state of the water droplet changes more intensely due to the greater temperature difference between the surrounding air and the droplet.

The experimental thermograms' graphs in Fig. 5, b and 5, c indicate that the dynamics of the thermal state of the ethanol and acetone droplets are similar to those of the water droplet. They are analogous to the effects of air temperature. Once in the experimental section, the experimental droplets of ethanol and acetone begin to warm up intensively until they reach an equilibrium evaporation state, and then their temperature stabilises. However, tested liquid droplets heat to different temperature t_e values. This is due to the nature and properties of the individual liquid. For example, at 100°C of air temperature, the droplet temperature t_e is about 17.8°C for acetone, about 32.3°C for ethanol, and 43.4°C for water.

The comparison of the data in Fig. 5 also indicates that the time of the transient phase change differs. It is observed that the acetone droplet warms to its equilibrium evaporating state more quickly. This is due to the values of the boiling temperature, latent heat, and specific heat of acetone being the lowest among the studied liquids. For example, at air temperature of 20°C, the latent heat of acetone is approximately 1.65 times and 4.63 times lower than that of ethanol and water, respectively. Thus, the smallest amount of thermal energy needs to be provided to the acetone droplet so that it begins to evaporate, and its vapour easily diffuses into the surrounding air.

As this work is focused on the analysis of the initial stages of droplet phase changes, the obtained results of droplet size change of water, ethanol, and acetone droplets are presented in the form of dimensionless average diameters in Fig. 6. These data show that the dynamics of change in droplet size during transient regimes are analogous for all studied liquids. Still, the specifics depend on the liquid itself. All tested liquid droplets immediately begin to decrease as they enter the experimental section. This shows that in all the cases studied, no condensation of water vapour on the surface of the experimental droplets has occurred, and the evaporation process of the liquid has been taking place from the beginning. Additionally, this suggests that droplet evaporation during the transient phase change is intense enough to compensate for the increase in droplet size resulting from liquid thermal expansion. The presented data in Fig. 6 also clearly demonstrate that the experimental droplet size of all liquids decreases rapidly with increasing airflow temperature. This is caused by more intense external heating in the hotter air flow.

Comparing the curves in Fig. 6, it is seen that under the same conditions, water droplets decrease at the slowest rate of all the liquids tested, while ethanol droplets decrease at the fastest rate. For example, at $\tau = 4$ s, in air at 100°C, the droplet diameter is approximately 15% for acetone, approximately 9.5% for ethanol, and only approximately 1.5% for water smaller than at the initial time point of placing the droplet in the experimental section. This is due to the nature of the materials. The thermal energy amount needed to warm acetone and ethanol droplets is considerably less than in the case of water (Table 1, values of specific heat cp), and acetone requires less thermal energy to evaporate (Table 1, values of latent heat L). Additionally, both of these liquids, especially acetone, possess inherent volatile properties. This causes their vapours to diffuse into the surrounding air faster than water.

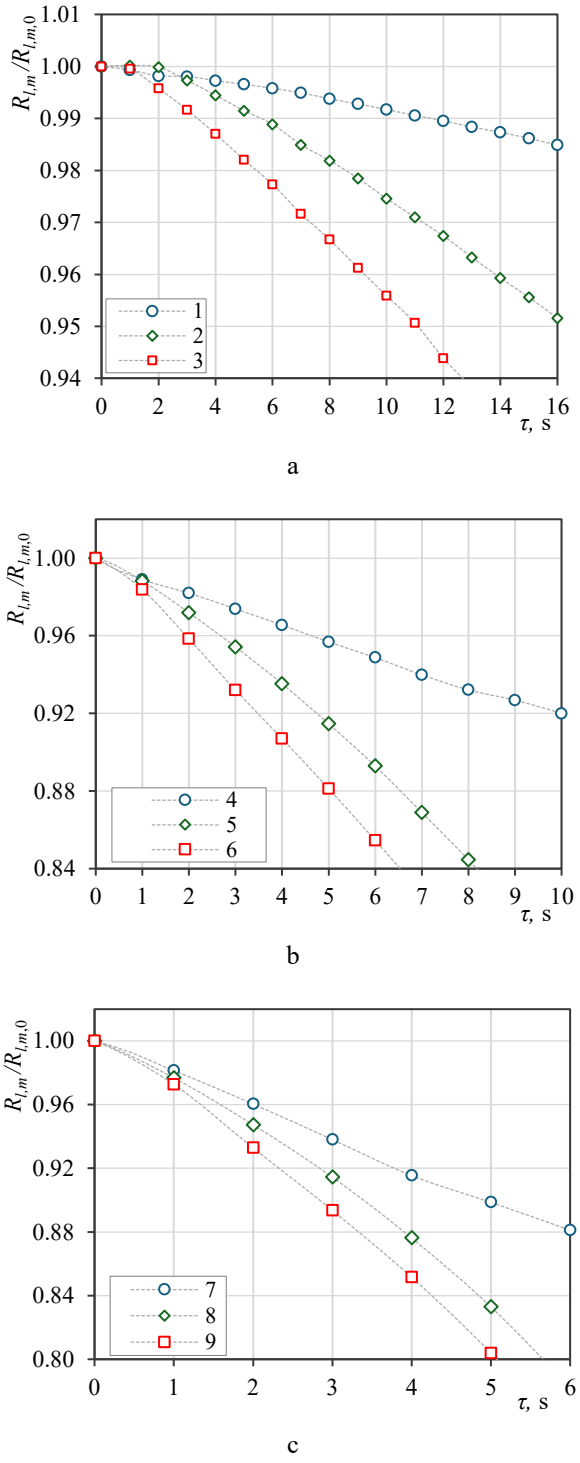

Fig. 6 The change of the experimental droplet dimensionless average diameter in the initial stages of phase change: a – water, b – ethanol and c – acetone; boundary conditions as given in Fig. 5

To make the data from experiments with water, ethanol and acetone easily applicable in practice, the liquid volumetric change rate and vapour mass flux were estimated according to expressions (3) and (4), respectively. The data of changes on the experimental droplets volume and vapour

flux obtained at air temperatures of 50°C and 100°C is presented in comparison graphs in Fig. 7 and Fig. 8.

The presented data in Fig. 7 demonstrate that in all cases, the volume of droplets decreases. This indicates that evaporative processes of liquid predominate in the transient phase change regimes. As evident from the data, the volume of the experimental liquid droplets decreases intensively with increasing air flow temperature. When the atmospheric

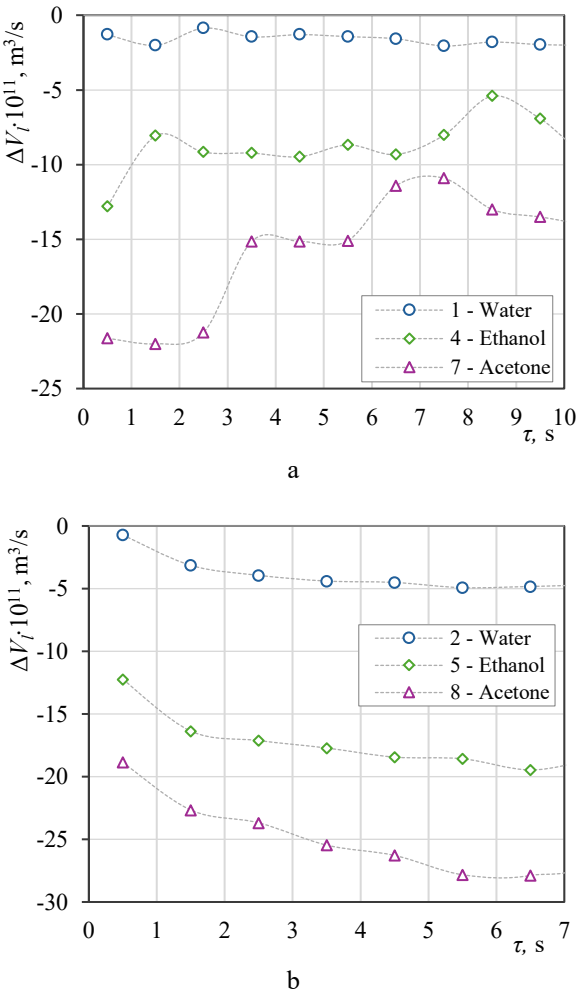

Fig. 7 The change of the volume of the experimental liquid droplet in the initial stages of the phase change. The air flow temperature is a – 50°C; b – 100°C; boundary conditions as given in Fig. 5

air is heated to 100°C, the highest module value of the volumetric change rate is higher by approximately $2.8 \cdot 10^{-11}$ m³/s for water, approximately $5.7 \cdot 10^{-11}$ m³/s for ethanol and approximately $6.9 \cdot 10^{-11}$m³/s for acetone compared with cases at 50°C air. Both graphs in Fig. 7 illustrate that in all cases the water droplet evaporates the weakest, while the acetone droplet evaporates the strongest. This again is determined by the nature and properties of the individual liquid (discussed earlier). For example, at the airflow of 100°C (Fig. 7, b), the maximum negative volume change in experimental droplet during evaporation for acetone is approximately 1.5 and 5.8 times larger than that of ethanol and water, respectively, under the same conditions.

The results of the vapour mass flux calculation of the tested liquid droplets at the initial stages of phase change are given in Fig. 8. In all cases, the vapour flux from the heated experimental droplet is positive – this demonstrates that only the evaporation process is occurring on the surface of tested liquids droplets. This is because the initial temperature of the liquid droplets is higher than the dew point temperature of the surrounding air. As can be seen from the data, the vapour flux of the evaporating droplet increases with the increasing surrounding airflow temperature. When the airflow is heated to 100°C, the maximum vapour flux generated is higher by approximately $2.7 \cdot 10^{-8}$ kg/s for water, approximately $4.2 \cdot 10^{-8}$ kg/s for ethanol and approximately $4.6 \cdot 10^{-8}$ kg/s for acetone compared with cases at 50°C airflow. The graphs presented in Fig. 8 indicates that the trends in the vapour flux of tested liquid droplets are very similar, while at the same time exhibiting unique characteristics determined by the nature of the liquid. For all tested liquid the vapour flux in the transitional evaporation mode increases to a maximum, remains almost constant at the beginning of the equilibrium evaporation regime and decreases as the diameter of the droplet rapidly diminishes. The highest vapor flow is generated in the case of acetone, which has strong volatile properties. When the airflow is heated to 100°C, the maximum vapour flux for acetone is approximately 1.5 and 4.5 times larger than that of ethanol and water, respectively.

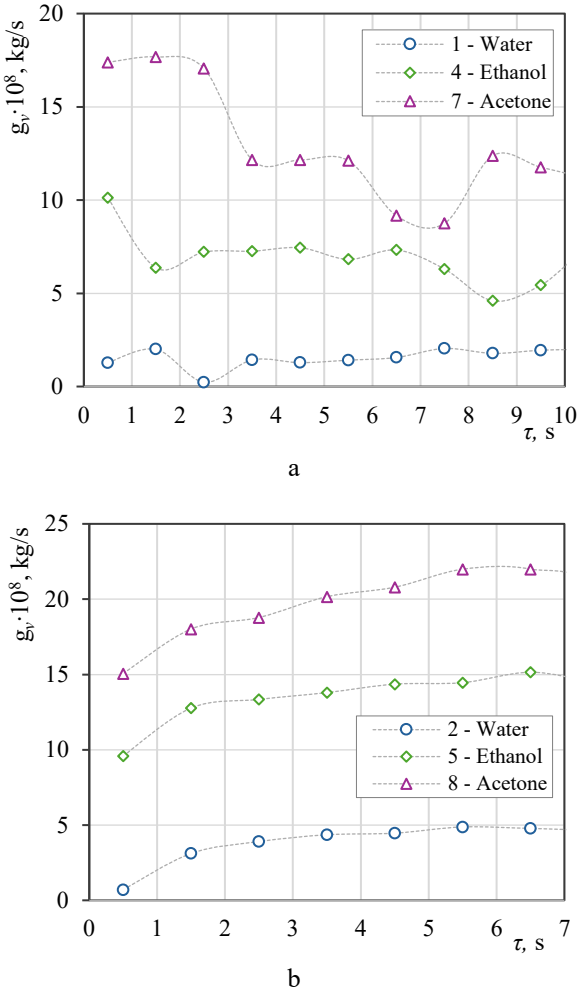

Fig. 8 The change of the vapour mass flux of the experimental liquid droplet in the initial stages of the phase change. The air flow temperature is a – 50°C; b – 100°C; boundary conditions as given in Fig. 5

4. Conclusions

The conducted experimental investigation on heat

transfer and phase changes of suspended water, ethanol and acetone droplets in the heated air flow at temperatures up to 130°C led to the following conclusions:

1. It was experimentally demonstrated that airflow temperature is a factor determining the thermal state variation of the water, ethanol and acetone droplets. Higher airflow temperatures allow studied fluid droplets to heat up faster in the transient evaporation regime and reach a higher equilibrium temperature. In heated air up to 50°C, the droplets equilibrium temperatures are approximately 8.5°C for acetone, 22.2°C for ethanol and 28.3°C for water. In 100°C air, these values become approximately 17.8°C, 32.3°C and 43.4°C, respectively.
2. The impact of the airflow temperature on the droplet temperature and evaporation rate of different liquids is qualitatively similar but quantitatively different for each liquid tested. Experiments have shown that the acetone droplet with the highest volatility has the lowest equilibrium evaporation temperature, and its transient processes occur most rapidly under all tested air cases.
3. Experiments performed show that under the studied conditions, droplets of all tested liquids evaporate quite strongly in the transient phase change regimes, leading to a decrease in the experimental droplet size from the very beginning.
4. The results show that the evaporation rate of all the liquid droplets tested increases with higher air temperatures. For all airflow boundary conditions tested, the liquid volumetric change and vapour mass flux of acetone droplets are highest. In the airflow heated to 100°C, the maximum vapour flux for acetone is approximately 1.5 and 4.5 times larger than that of ethanol and water, respectively.
5. The analysis of experimental data suggests that liquids with strong volatile properties and low boiling points, such as the tested liquid acetone, could be attractive as adequate working fluids for low-temperature spray cooling.

References

1. **Qubeissi, M. A.** 2018. Predictions of droplet heating and evaporation: An application to biodiesel, diesel, gasoline and blended fuels, Applied Thermal Engineering 136: 260-267. https://doi.org/10.1016/j.applthermaleng.2018.03.010.
2. **Faik, A. M. D.; Zhang, Y.** 2020. Liquid-phase dynamics during the two-droplet combustion of diesel-based fuel mixtures, Experimental Thermal and Fluid Science 115: 110084. https://doi.org/10.1016/j.expthermflusci.2020.110084.
3. **Poonawala, T.; Muelas, A.; Ballester, J.** 2024. Evaporation and combustion of low asphaltene heavy oil droplets under conditions representative of practical applications, Energy 313: 133765. https://doi.org/10.1016/j.energy.2024.133765.
4. **Fedorenko, R. M.; Yanovsky, L. S.; Strizhak, P. A.** 2025. The effect of micro-explosive fragmentation of water-fuel droplets on their spray combustion emissions, Fuel 396: 135344. https://doi.org/10.1016/j.fuel.2025.135344.
5. **Pawlak-Kruczek, H.; Ostrycharczyk, M.; Zgora, J.** 2013. Co-combustion of liquid biofuels in PC boilers of 200 MW utility unit, Proceedings of the Combustion Institute 34(2): 2769-2777. https://doi.org/10.1016/j.proci.2012.08.010.
6. **Lindfors, Ch.; Oasmaa, A.; Välimäki, A.; Ohra-aho, T.; Punkkinen, H.; Bajamundi, C.; Onarheim, K.** 2019. Standard liquid fuel for industrial boilers from used wood, Biomass and Bioenergy 127: 105265. https://doi.org/10.1016/j.biombioe.2019.105265.
7. **Zhao, L. M.; Zhangn, Y. M.; Zhao, H. Z.; Fang, J.; Qin, J.** 2014. Numerical case studies of vertical wall fire protection using water spray, Case Studies in Thermal Engineering 4: 129-135. https://doi.org/10.1016/j.csite.2014.09.002.
8. **Li, Y. Z.; Ingason, H.; Arvidson, M.; Forsth, M.** 2024. Performance of various water-based fire suppression systems in tunnels with longitudinal ventilation, Fire Safety Journal 146: 104141. https://doi.org/10.1016/j.firesaf.2024.104141.
9. **Ha, G.; Shin, W. G.; Lee, J.** 2021. Numerical analysis to determine fire suppression time for multiple water mist nozzles in a large fire test compartment, Nuclear Engineering and Technology 53(4): 1157-1166. https://doi.org/10.1016/j.net.2020.09.028.
10. **Noaki, M.; Delichatsios, M. A.; Yamaguchi J., Ohmiya, Y.** 2018. Heat release rate of wooden cribs with water application for fire suppression, Fire Safety Journal 95: 170-179. https://doi.org/10.1016/j.firesaf.2017.10.002.
11. **Yang, H.; Pei, N.; Fan, M.; Liu, L., Wang, D.** 2021. Experimental study on an air-cooled air conditioning unit with spray evaporative cooling system, International Journal of Refrigeration 131: 645-656. https://doi.org/10.1016/j.ijrefrig.2021.06.011.
12. **Charoensin-O-larn, R.; Kavee, N.; Klinbun, J.** 2024. Experimental study on the influence of the water spray cooling on air-cooled condenser of the split-type air conditioner, Case Studies in Thermal Engineering 61: 104941. https://doi.org/10.1016/j.csite.2024.104941.
13. **Stefaniak, Ł.; Walaszczyk, J.; Danielewicz, J.; Rajski K.** 2025. Experimental performance analysis of non-porous indirect evaporative coolers under intermittent water spraying conditions, Journal of Building Engineering 105: 112585. https://doi.org/10.1016/j.jobe.2025.112585.
14. **Alkhedhair, A.; Guan, Z.; Jahn, I.; Gurgenci, H.; He, S.** 2015. Water spray for pre-cooling of inlet air for Natural Draft Dry Cooling Towers − Experimental study, International Journal of Thermal Sciences 90: 70-78. https://doi.org/10.1016/j.ijthermalsci.2014.11.029.
15. **Wang, Z.; Xing, Y.; Liu, X.; Zhao, L.; Ji, Y.** 2016. Computer modeling of droplets impact on heat transfer during spray cooling under vibration environment, Applied Thermal Engineering 107: 453-462. https://doi.org/10.1016/j.applthermaleng.2016.06.176.
16. **Farooq, W.; Suh, W. I.; Park, M. P.; Yang, J. W.** 2015. Water use and its recycling in microalgae cultivation for biofuel application, Bioresource Technology 184: 73-81. https://doi.org/10.1016/j.biortech.2014.10.140.
17. **Miliauskas, G.; Maziukienė, M.; Jouhara, H.; Poskas, R.** 2019. Investigation of mass and heat transfer transitional processes of water droplets in wet gas flow

in the framework of energy recovery technologies for biofuel combustion and flue gas removal, Energy 173: 740-754. https://doi.org/10.1016/j.energy.2019.02.101.

18. **Larki, I.; Zahedi, A.; Asadi, M.; Forootan, M. M.; Farajollahi, M.; Ahmadi, R.; Ahmadi, A.** 2023. Mitigation approaches and techniques for combustion power plants flue gas emissions: A comprehensive review, Science of the Total Environment 903: 166108. https://doi.org/10.1016/j.scitotenv.2023.166108.
19. **Miliauskas, G.; Pabarčius, R.; Maziukienė, M.** 2022. Uncertainty and sensitivity analysis of boundary conditions during water droplet phase change regimes, International Journal of Thermal Sciences 171: 107228. https://doi.org/10.1016/j.ijthermalsci.2021.107228.
20. **Chen, H.; Ruan, X. H.; Peng, Y. H.; Wang, Y. L.; Yu, C. K.** 2022. Application status and prospect of spray cooling in electronics and energy conversion industries, Sustainable Energy Technologies and Assessments 52: 102181. https://doi.org/10.1016/j.seta.2022.102181.
21. **Hsieh, S. S.; Chen, G. W.; Yeh, Y. F.** 2015. Optical flow and thermal measurements for spray cooling, International Journal of Heat and Mass Transfer 87: 248-253. https://doi.org/10.1016/j.ijheatmasstransfer.2015.04.005.
22. **Kandasamy, R.; Ho, J. Y.; Liu, P. F.; Wong, T. N.; Toh, K. C.; Chua, S. Jr.** 2022. Two-phase spray cooling for high ambient temperature data centers: Evaluation of system performance, Applied Energy 305: 117816. https://doi.org/10.1016/j.apenergy.2021.117816.
23. **Wang, Y.; Liu, M.; Liu, D.; Xu, K.; Chen, Y.** 2010. Experimental study on the effects of spray inclination on water spray cooling performance in non-boiling regime, Experimental Thermal and Fluid Science 34(7): 933-942. https://doi.org/10.1016/j.expthermflusci.2010.02.010.
24. **Liu, X.; Liu, L.; Li, R.; Xie, J.; Wang, Z.** 2025. Research on the performance and application of spray cooling in the gas phase space, Thermal Science and Engineering Progress 59: 103383. https://doi.org/10.1016/j.tsep.2025.103383.
25. **Fuchs, N. A.** 1959. Evaporation and droplet growth in gaseous media. London: Pergamon Press. 72p. https://doi.org/10.1016/B978-1-4832-0060-6.50002-8.
26. **Sazhin, S.** 2014. Droplets and Sprays. London: Springer. 345p. https://doi.org/10.1007/978-1-4471-6386-2.
27. **Miliauskas, G.; Puida, E.; Poškas, R.; Ragaišis, V.; Paukštaitis, L.; Jouhara H.; Mingilaitė, L.** 2022. Experimental investigations of water droplet transient phase changes in flue gas flow in the range of temperatures characteristic of condensing economizer technologies, Energy 256: 124643. https://doi.org/10.1016/j.energy.2022.124643.
28. **Volkov, R. S.; Strizhak, P. A.** 2018. Research of temperature fields and convection velocities in evaporating water droplets using Planar Laser-Induced Fluorescence and Particle Image Velocimetry, Experimental Thermal and Fluid Science 97: 392-407. https://doi.org/10.1016/j.expthermflusci.2018.05.007.
29. **Zhou, Q.; Erkan, N.; Okamoto, K.** 2019. Simultaneous measurement of temperature and flow distributions inside pendant water droplets evaporating in an upward air stream using temperature-sensitive particles, Nuclear Engineering and Design 345: 157-165. https://doi.org/10.1016/j.nucengdes.2019.02.019.
30. **Piskunov, M.; Strizhak, P.; Volkov, R.** 2021. Experimental and numerical studies on the temperature in a pendant water droplet heated in the hot air, International Journal of Thermal Science163: 106855. https://doi.org/10.1016/j.ijthermalsci.2021.106855.
31. **Antonov, D. V.; Tonini, S.; Cossali, G. E.; Strizhak, P. A.; Sazhin, S. S.** 2024. Heating and evaporation of a mono-component spheroidal droplet with non-uniform surface temperature, Applied Mathematical Modelling 125: 687-703. https://doi.org/10.1016/j.apm.2023.10.019.
32. **Ramanauskas, V.; Puida, E.; Miliauskas, G.; Paukštaitis, L.** 2019. Experimental investigation of water droplet heating in humidified air flow, Mechanika 25(6): 434-441. https://doi.org/10.5755/j01.mech.25.6.23795.
33. **Miliauskas, G.; Maziukienė, M.; Poškas, R.; Jouhara H.** 2024. Peculiarities of thermal and energy state variation in phase change regimes of water droplets in radiating biofuel flue gas flow, Energy 307: 132620. https://doi.org/10.1016/j.energy.2024.132620.
34. **Liu, H.; Cai, C.; Yin, H.; Luo, J.; Jia, M.; Gao, J.** 2018. Experimental investigation on heat transfer of spray cooling with the mixture of ethanol and water, International Journal of Thermal Sciences 133: 62-68. https://doi.org/10.1016/j.ijthermalsci.2018.07.018.
35. **Terekhov, V. I.; Karpov, P. N.; Nazarov, A. D.; Serov A. F.** 2020. Unsteady heat transfer at impinging of a single spray pulse with various durations, International Journal of Heat and Mass Transfer 158: 120057. https://doi.org/10.1016/j.ijheatmasstransfer.2020.120057.
36. **Panão, M. R. O.; Moreira, A. L. N.** 2009. Intermittent spray cooling: A new technology for controlling surface temperature, International Journal of Heat and Fluid Flow 30(1): 117-130. https://doi.org/10.1016/j.ijheatfluidflow.2008.10.005.
37. **Bhatt, N. H.; Pati, A. R.; Kumar, A.; Behera, A.; Munshi, B.; Mohapatra, S. S.** 2017. High mass flux spray cooling with additives of low specific heat and surface tension: A novel process to enhance the heat removal rate, Applied Thermal Engineering 120: 537-548. https://doi.org/10.1016/j.applthermaleng.2017.03.137.
38. **Putra, I. K. G. T. A.; Nguyen, H. X. D.; Tran, Q. K.; Lim, O.** 2025. Optical and computational investigations: Assessing the impact of absolute ethanol mixtures on diesel spray behavior, Fuel 390: 134756. https://doi.org/10.1016/j.fuel.2025.134756.
39. **Alahmer, H.; Alahmer, A.; Alkhazaleh, R.; Alrbai, M.** 2023. Exhaust emission reduction of a SI engine using acetone–gasoline fuel blends: Modeling, prediction, and whale optimization algorithm, Energy Reports 9(1): 77-86. https://doi.org/10.1016/j.egyr.2022.10.360.
40. **Han, K.; Pang, B.; Zhao, C.; Ni, Z.; Qi, Z.** 2019. An experimental study of the puffing and evaporation characteristics of acetone-butanol-ethanol (ABE) and diesel blend droplets, Energy 183: 331-340. https://doi.org/10.1016/j.energy.2019.06.068.
41. **Dong, Q.; Liu, C.; Lai, C.; Lin, J.; Zhao, J.; Liu, M.**

2024. Experimental study on the dynamics characteristics of biodiesel/ethanol droplets impacting upon the heated wall, International Communications in Heat and Mass Transfer 159: 108038. https://doi.org/10.1016/j.icheatmasstransfer.2024.108038.

42. **Biknienė, K.; Paukštaitis, L.** 2024. Averaged heat fluxes densities during condensation and evaporation of a water droplet, Mechanika 30(2): 150-158. https://doi.org/10.5755/j02.mech.35522.

K. Biknienė

EXPERIMENTAL INVESTIGATION OF SUSPENDED WATER, ETHANOL AND ACETONE TRANSIENT PHASE CHANGE REGUMES IN THE HEATED AIRFLOW

S u m m a r y

This paper presents an experimental investigation into the use of water, ethanol, and acetone using the suspended droplet method. The influence of atmospheric air temperatures on droplets in the transient phase change is analysed. Experimental results are presented, including thermograms that characterise the droplet's thermal state and diameter monograms that define the variation in droplet size. These data are processed according to the droplet liquid volume change rate parameter. The experimental results confirm that the airflow temperature leads to intensified heat exchange and phase change processes during the droplet transition stages, resulting in the droplet's heating to a higher thermal equilibrium evaporation state. For all the fluids studied, the impact of airflow temperature on the droplet temperature and liquid volume change rate of different liquids is qualitatively similar. Still, the strength of the influence varies depending on the nature and properties of the liquid. In heated air up to 50°C, the droplet equilibrium temperatures are approximately 8.5°C for acetone, 22.2°C for ethanol and 28.3°C for water. In 100°C air, these values become approximately 17.8°C, 32.3°C and 43.4°C, respectively. The estimated volume change in the liquid droplet's size and vapour mass flux show that acetone, which has the most volatile properties and lowest boiling temperature, evaporates most intensely from the liquids tested in the initial stage.

Keywords: experimental investigation; water, ethanol, acetone droplets; evaporation; transient phase change.

Received May 31, 2025
Accepted August 22, 2025